

Joint estimation of cosmological parameters from CMB and IRAS data

Matthew Webster¹

Institute of Astronomy, Madingley Road, Cambridge CB3 0HA, UK

M.P. Hobson and A.N. Lasenby

Mullard Radio Astronomy Observatory, Cavendish Labs, Madingley Road, Cambridge CB3 0HE

Ofer Lahav

Institute of Astronomy, Madingley Road, Cambridge CB3 0HA, UK

and

Graça Rocha

Department of Physics, Kansas State University, Manhattan, KS 66506, USA

ABSTRACT

Observations of large scale structure (LSS) and the cosmic microwave background (CMB) each place separate constraints on the values of cosmological parameters. We calculate a joint likelihood based on various CMB experiments and the IRAS 1.2 Jy galaxy redshift survey and use this to find an overall optimum. Our formulation self-consistently takes account of the underlying mass distribution, which affects both the CMB potential fluctuations and the IRAS redshift distortion. This not only allows more accurate parameter estimation, but also removes the parameter degeneracy which handicaps calculations based on either approach alone. The family of Cold Dark Matter (CDM) models analysed corresponds to a spatially-flat universe with an initially scale-invariant spectrum and a cosmological constant. Free parameters in the joint model are the mass density due to all matter (Ω_m), baryonic density (Ω_b), Hubble's parameter ($h = H_0/100 \text{ km s}^{-1}$), IRAS light-to-mass bias (b_{iras}) and the variance in the galaxy field measured in an $8 h^{-1}\text{Mpc}$ radius sphere (σ_8). Results from the two data sets show good agreement, and the joint optimum lies at $\Omega_m = 0.32 \pm 0.08$, $\Omega_b = 0.061 \pm 0.013$, $h = 0.47 \pm 0.06$, $\sigma_8 = 0.78 \pm 0.10$, $b_{\text{iras}} = 1.04 \pm 0.06$ (marginalised error bars correspond to 95 percent confidence).

Subject headings: Cosmic microwave background, Large-scale structure

¹email: mwebster@ast.cam.ac.uk

1. Introduction

Astronomical observations allow us to evaluate cosmological models, and determine likely values for the parameters within them. As the variety and depth of these observations have improved, so too have the techniques for comparing them against theoretical predictions.

Observations of anisotropies in the cosmic microwave background (CMB) provide one of the key constraints for cosmological models and a significant quantity of experimental data already exists. By comparing the power spectrum of the CMB fluctuations derived from these experiments with the power spectra predicted by different cosmological models it is possible to set constraints on the value of certain cosmological parameters (Hancock et al. 1998, Rocha et al. (in preparation), Lineweaver et al. 1997).

Galaxy redshift surveys, mapping large scale structure (LSS), provide another cosmologically important set of observations. The clustering of galaxies in redshift-space is systematically different from that in real-space (Kaiser 1987). The mapping between the two is a function of the underlying mass distribution, in which the galaxies are not only tracers, but also velocity test particles (Lahav 1996). Many techniques have been developed for estimating this mapping (Yahil et al. 1991, Kaiser et al. 1991). Statistical quantities can be generated for a given cosmology and these used to constrain model parameters through comparison with survey data (Fisher, Scharf & Lahav 1994, Cole et al. 1995, Heavens & Taylor 1995, Fisher & Nusser 1996, Willick et al. 1997).

Estimates derived separately from each of these two data sets have problems with parameter degeneracy. In the analysis of LSS data, there is uncertainty as to how well the observed light distribution traces the underlying mass distribution. The light-to-mass bias, b , introduced to account for this uncertainty, affects the value of many central cosmological parameters, and makes any identified optimum degenerate (Strauss & Willick 1995). Similarly, on the basis of CMB data alone, there is considerable degeneracy (Bond et al. 1995c) between $h = H_0/100 \text{ km s}^{-1}\text{Mpc}^{-1}$ and the energy density Ω_Λ due to the cosmological constant (Carroll, Press & Turner 1992). This leads to poor estimation of the baryon (Ω_b) and total mass (Ω_m) densities (Lineweaver et al. 1997).

In this letter, we combine results from a bandpower approach covering a range of CMB experiments, with a likelihood analysis of the IRAS 1.2Jy survey, performed in spherical harmonics. To our knowledge, this is the first self-consistent formulation of CMB and LSS parameter estimation. In particular, our method expresses the effects of the underlying mass distribution on both the CMB potential fluctuations and the IRAS redshift distortion. This breaks the degeneracy inherent in an isolated analysis of either data set, and places tight constraints on several cosmological parameters. Indeed, it is unsurprising that the two data sets are complimentary, given that they sample our universe at extreme ends of its evolution.

For simplicity, we restrict our attention to inflationary, cold dark matter (CDM) models, assuming a flat universe with linear, scale-independent biasing.

2. CMB Parameter Estimation

2.1. Experimental Data

Since the discovery of CMB fluctuations by the COBE satellite (Smoot et al. 1992, Bennett et al. 1996), several other experiments have also measured CMB anisotropies over a wide range of angular scales. These experiments include ground-based beam-switching experiments such as Tenerife (Hancock et al. 1997, Hancock et al. 1994), Python (Ruhl et al. 1995), South Pole (Gundersen et al. 1995) and Saskatoon (Netterfield et al. 1997); balloon-bourne instruments such as ARGO (De Bernardis et al. 1994), MAX (Tanaka et al. 1996), and MSAM (Cheng et al. 1994, Cheng et al. 1996) and the ground-based interferometer CAT (Scott et al. 1996).

These observations have resulted in a first estimate of the CMB power spectrum and they are discussed in more detail by Hancock et al. 1998. In particular, Hancock et al. display the window function W_l for each experiment and convert the level of anisotropy observed in each case to flat bandpower estimates $(\Delta T_l/T) \pm \sigma$ centred on the effective multipole l_{eff} of the corresponding window function (see below). The resulting CMB data points are plotted in Fig. 1, together with their 68 per cent confidence limits. These confidence limits have been obtained using likelihood analyses and hence incorporate uncertainties due to random errors, sampling variance (Scott, Srednicki and White 1994) and cosmic variance (Scaramella & Vittorio 1990, Scaramella & Vittorio 1993). A discussion of possible additional uncertainties due to contamination by foreground emission is given by Rocha et al. (in preparation).

The data points plotted in Fig. 1 differ slightly from those given in Hancock et al. 1998, since the Saskatoon points have been increased by 7 per cent, as suggested by the recent investigation of systematic calibration errors in the Saskatoon experiment (Leitch, private communication).

2.2. Method

Temperature fluctuations in the CMB are usually described in terms of the spherical harmonic expansion

$$\frac{\Delta T(\theta, \phi)}{T} = \sum_{l=0}^{\infty} \sum_{m=-l}^l a_{lm} Y_{lm}(\theta, \phi) , \quad (1)$$

from which we define the ensemble-average CMB power spectrum $C_l = \langle |a_{lm}|^2 \rangle$. Alternatively, we may describe the fluctuations in terms of their autocorrelation function

$$C(\theta) = \frac{1}{4\pi} \sum_{l=2}^{\infty} (2l+1) C_l P_l(\cos \theta) . \quad (2)$$

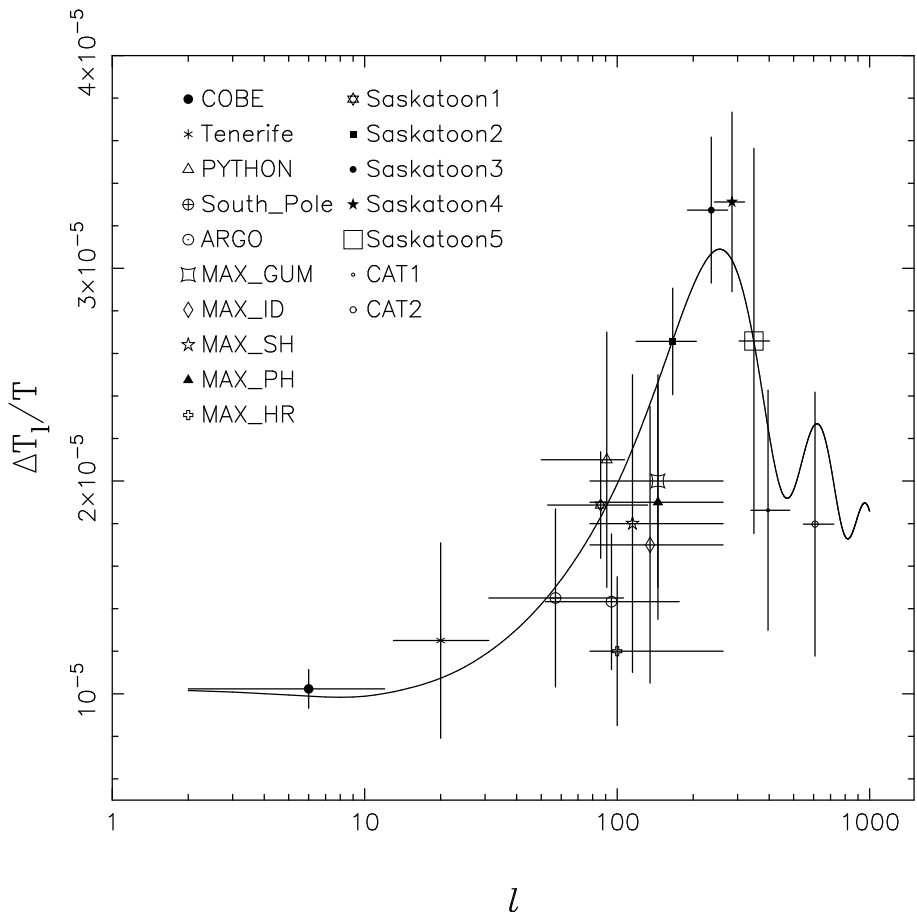


Fig. 1.— The data points used in the calculation of the CMB likelihood function. The overlaid curve is generated on the basis of the joint optimum derived in this paper.

The power in the CMB fluctuations observed by an experiment with window function W_l is then given by

$$C_{\text{obs}}(0) = \left\langle \left(\frac{\Delta T_{\text{obs}}}{T} \right)^2 \right\rangle = \frac{1}{4\pi} \sum_{l=2}^{\infty} (2l+1) C_l W_l , \quad (3)$$

and for each experiment we define the flat bandpower by

$$\frac{\Delta T_l}{T} = \sqrt{\frac{C_{\text{obs}}(0)}{I(W_l)}} , \quad (4)$$

where $I(W_l)$ is defined (Bond 1995a, Bond 1995b) as

$$I(W_l) = \sum_{l=2}^{\infty} \frac{(l + \frac{1}{2})}{l(l+1)} W_l . \quad (5)$$

This flat bandpower estimate is centred on the effective multipole

$$l_{\text{eff}} = \frac{I(l W_l)}{I(W_l)} . \quad (6)$$

We wish to compare these bandpower estimates with those predicted by different cosmological models. Varying the values of model parameters, we calculate corresponding, predicted CMB power spectrum C_l , using the Boltzmann code of Seljak & Zaldarriaga Seljak & Zaldarriaga 1996. This is then used to calculate the predicted flat bandpower ΔT_l for each experiment. The chi-squared statistic for a given set of parameter values, $\vec{\alpha}_{\text{cmb}}$, is then

$$\chi^2(\vec{\alpha}_{\text{cmb}}) = \sum_{i=1}^{N_d} \frac{1}{\sigma_i^2} \left(\left[\Delta T_l^{\text{obs}} \right]_i - \left[\Delta T_l^{\text{pred}}(\vec{\alpha}_{\text{cmb}}) \right]_i \right)^2 , \quad (7)$$

where N_d is the number of CMB data points plotted in Fig. 1 (17 in this analysis). Moreover, since the CMB data points plotted in the Fig. 1 were chosen such that no two bandpower estimates come from experiments which observed overlapping patches of sky and had overlapping window functions, we may consider them as *independent* estimates of the CMB power spectrum. Given this, the determinant in the likelihood function is constant, and hence the an unnormalised likelihood is given simply by $\mathcal{L}_{\text{cmb}} \propto e^{-\chi^2/2}$.

As mentioned above, we assume that the Universe is spatially flat, and that there are no tensor contributions to the CMB power spectrum. We take the primordial scalar perturbations to be described by the Harrison-Zel'dovich power spectrum for which $n_s = 1$, and further assume that the optical depth to the last scattering surface is zero.

The normalisation of the CMB power spectrum is determined by Q , which gives the strength of the quadrupole in μK , such that

$$C_2 = \frac{4\pi}{5} \left(\frac{Q}{T_0} \right)^2 , \quad (8)$$

where T_0 is the average CMBR temperature. The expansion rate of the Universe is given by Hubble's parameter $h = H_0/100$ km s $^{-1}$, while Ω_{cdm} and Ω_b denote the density of the Universe in CDM and the baryons respectively, each in units of the critical density. Given that we assume a flat universe, but investigate models where

$$\Omega_m \equiv (\Omega_{\text{cdm}} + \Omega_b) < 1 , \quad (9)$$

the shortfall is made up through a non-zero cosmological constant Λ such that

$$\Omega_\Lambda = 1 - \Omega_m = \frac{\Lambda}{3H_0^2} . \quad (10)$$

Thus we consider the reduced set of CMB parameters

$$\vec{\alpha}_{\text{cmb}} \equiv \{Q, h, \Omega_{\text{cdm}}, \Omega_b\} . \quad (11)$$

In Section 4, we derive a set of joint parameters linking these to the IRAS parameter set.

3. IRAS Parameter Estimation

3.1. IRAS 1.2Jy Survey

The IRAS surveys are uniform and complete down to Galactic latitudes as low as $\pm 5^\circ$ from the Galactic plane. This makes them ideal for estimating whole-sky density and velocity fields. Here, we use the 1.2 Jy IRAS survey (Fisher et al. 1995), consisting of 5313 galaxies, covering 87.6% of sky with the incomplete regions being dominated by the 8.7% of the sky with $|b| < 5^\circ$.

In principle, the method we are using can be extended to account explicitly for the incomplete sky coverage. However, we adopt the simpler approach of smoothly interpolating the redshift distribution over the missing areas (Yahil et al. 1991). The effects of this interpolation on the computed harmonics have been shown to be negligible (Lahav et al. 1994).

3.2. Method

In this letter, we assume linear, scale-independent biasing, where b_{iras} measures the ratio between fluctuations in the IRAS galaxy distribution and the underlying mass density field:

$$(\delta\rho/\rho)_{\text{iras}} = b_{\text{iras}} (\delta\rho/\rho)_m . \quad (12)$$

The velocity and density fields in linear theory (Peebles 1980), are linked by a proportionality factor β_{iras} , such that

$$\nabla \cdot \mathbf{v} = -H_0 \beta_{\text{iras}} (\delta\rho/\rho)_m = -H_0 \left(\frac{\Omega_m^{0.6}}{b_{\text{iras}}} \right) (\delta\rho/\rho)_m . \quad (13)$$

Statistically, the fluctuations in the real-space galaxy distribution can be described by a power spectrum, $P_R(k)$, which is determined by the *rms* variance in the observed galaxy field, measured for an $8 h^{-1}$ Mpc radius sphere ($\sigma_{8,\text{iras}}$) and a shape parameter (e.g. Γ in equation 19). The observed $\sigma_{8,\text{iras}}$ is related to the underlying σ_8 for mass through the bias parameter, such that $\sigma_{8,\text{iras}} = b_{\text{iras}} \sigma_8$.

The approach we use in this letter follows Fisher, Scharf & Lahav (1994; hereafter FSL), and we include here only a brief introduction to our technique. FSL provides a detailed description of the spherical harmonic approach to parameter estimation.

A flux-limited, redshift-space density field can be decomposed into spherical harmonics Y_{lm} , with coefficients

$$a_{lm}^S = \sum_{i=1}^{N_g} f(s_i) Y_{lm}(\hat{\mathbf{s}}_i) , \quad (14)$$

where N_g is the number of galaxies in the survey, and $f(s)$ is an arbitrary radial weighting function—this process is analogous to Fourier decomposition, but instead using spherical basis functions. The sum over galaxies in this equation can be rewritten as a continuous integral of the density fluctuation field $\delta(\mathbf{s})$ over redshift-space:

$$a_{lm}^S = \int d^3\mathbf{s} \phi(r) f(s) [1 + \delta_S(\mathbf{s})] Y_{lm}(\hat{\mathbf{s}}) , \quad (15)$$

where $\phi(r)$ is the radial selection function of the survey, evaluated at the real-space distance of the i^{th} galaxy.

As detailed in FSL, assuming the perturbations introduced by peculiar velocities are small, the expected linear theory values for the harmonic coefficients are

$$\left\langle |a_{lm}^S|^2 \right\rangle_{\text{LT}} = \frac{2}{\pi} \int_0^\infty dk k^2 P_R(k) \left| \Psi_l^R(k) + \beta_{\text{iras}} \Psi_l^C(k) \right|^2 . \quad (16)$$

Here, Ψ^R is the real-space window function, while $\beta_{\text{iras}} \Psi^C$ is a “correction” term which embodies the redshift distortion.

For a given set of cosmological parameters, redshift-space harmonics a_{lm}^i can be calculated for different weighting functions $f^i(r)$, $i = 1, \dots, N$. If the underlying density field is Gaussian, on the basis of the coefficients predicted in equation 16, the likelihood of the survey harmonics can be calculated as

$$\mathcal{L}_{\text{iras}} \propto |\mathbf{A}|^{-\frac{1}{2}} \exp \left(-\frac{1}{2} [\vec{a}^T \mathbf{A}^{-1} \vec{a}] \right) . \quad (17)$$

Here \vec{a} is the vector of observed harmonics for different shells and \mathbf{A} is the corresponding covariance matrix, which depends on the predicted harmonics. In addition to the $\langle |a_{lm}^S|^2 \rangle_{\text{LT}}$ from equation 16, these predicted harmonics will also have a shot-noise contribution $\langle |a_{lm}^S|^2 \rangle_{\text{SN}}$ due to the discreteness of survey galaxies.

In this letter, we follow FSL and use four Gaussian windows centered at 38, 58, 78, and 98 $h^{-1}\text{Mpc}$ each with a dispersion of 8 $h^{-1}\text{Mpc}$. For each window, we compute the corresponding weighted redshift harmonics for the IRAS 1.2Jy catalog, and use these to determine the likelihood of a given set of parameter values. Since our analysis is valid only in the linear regime, we restrict the likelihood computation to $l_{\text{max}} = 10$. Hence, the IRAS likelihood function has a parameter vector

$$\vec{\alpha}_{\text{iras}} \equiv \{\beta_{\text{iras}}, \sigma_{8,\text{iras}}, \Gamma\} . \quad (18)$$

Again, the linkage between these and the CMB parameters is discussed in section 4 below.

4. Joint analysis

Given the large number of parameters available between the two models, it is important both to find links for joint optimisation, and to decide which parameters can be frozen. From section 3, we have seven variables between the two models: $\{Q, h, \Omega_{\text{cdm}}, \Omega_b, \beta_{\text{iras}}, \sigma_{8,\text{iras}}, \Gamma\}$. These can be reduced further by expression in terms of core cosmological parameters. The CMB normalisation can be calculated as $Q \equiv f(\Omega_m, \sigma_8, \Gamma)$ (Bardeen et al. 1986, Efstathiou, Bond & White 1995), while the CDM shape parameter is well-approximated (Sugiyama 1995) by

$$\Gamma = \Omega_m h \exp \left(-\Omega_b \left[1 + \frac{\sqrt{h/0.5}}{\Omega_m} \right] \right) . \quad (19)$$

Meanwhile, we have shown above that $\Omega_m = \Omega_{\text{cdm}} + \Omega_b$, $\beta_{\text{iras}} = \Omega_m^{0.6}/b_{\text{iras}}$, and $\sigma_{8,\text{iras}} = \sigma_8 b_{\text{iras}}$. Hence, the final, joint parameter space is

$$\vec{\alpha}_{\text{joint}} \equiv \{h, \sigma_8, \Omega_m, \Omega_b, b_{\text{iras}}\} . \quad (20)$$

Each of the CMB and IRAS data sets provides a likelihood function; hence the joint likelihood is given by

$$\ln(\mathcal{L}_{\text{joint}}) = \ln(\mathcal{L}_{\text{cmb}}) + \ln(\mathcal{L}_{\text{iras}}) . \quad (21)$$

The calculation of this likelihood for a given set of parameters is computationally expensive. However, the likelihood function is very well-behaved throughout the parameter range considered. Hence, standard multivariate optimisation techniques can be used (Press et al. 1992). A 95% confidence range is calculated for each variable by marginalisation over the remaining variables, reducing the probability distribution to a single dimension. The width of this confidence range is then used to estimate a symmetric error on the global optimal value.

5. Results

The results for the two separate data set are in good agreement, leading to a well-defined joint optimum. Table 1 shows the position of this optimum in terms of CMB, IRAS and

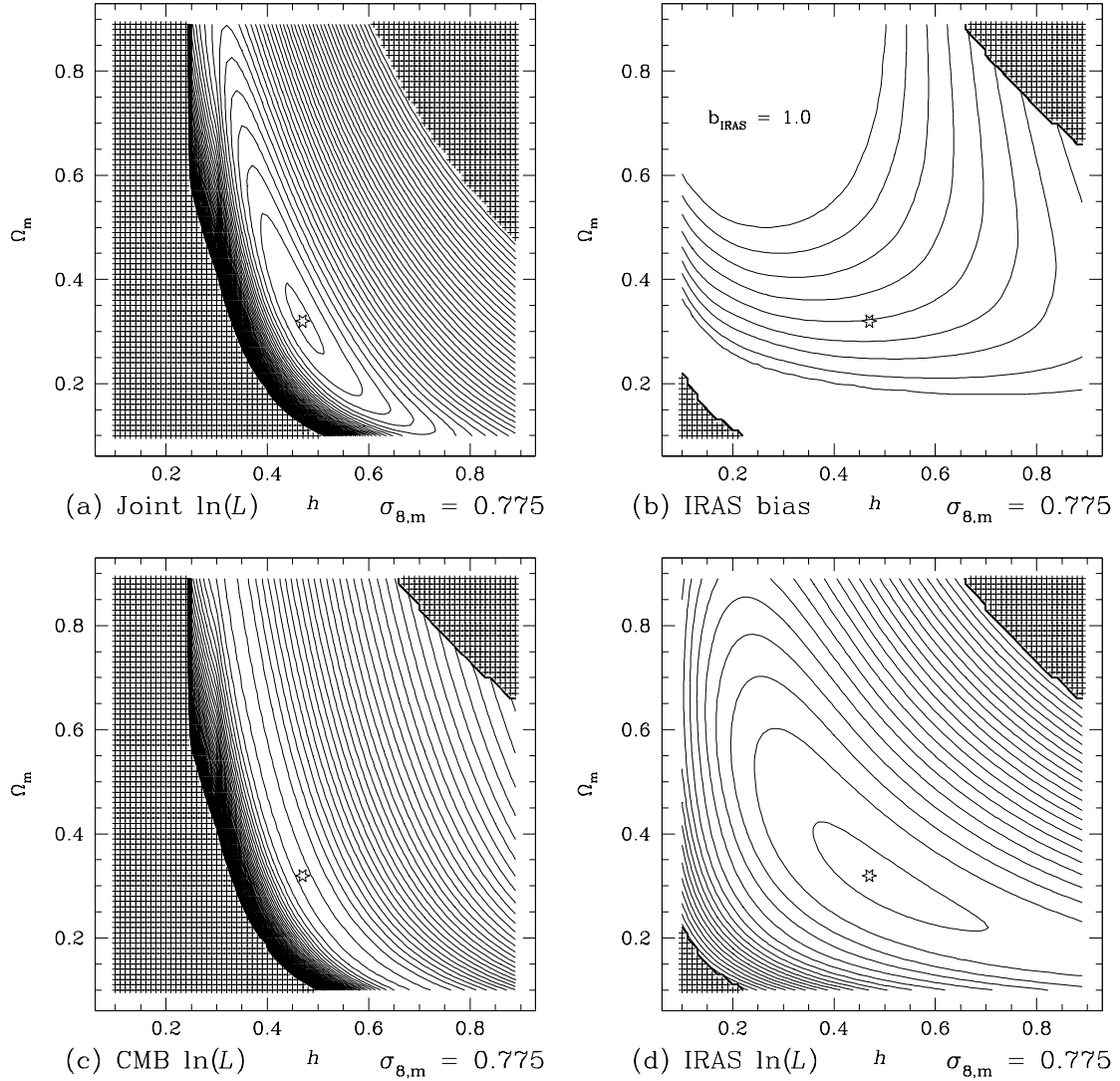


Fig. 2.— Plots on the $\{\Omega_m, h\}$ plane at the optimal value of $\sigma_8 = 0.775$, with joint optimum marked at $\Omega_m = 0.32$, $h = 0.47$. These plots show parameter degeneracy being broken using joint likelihood. (a) Joint likelihood, showing well-defined optimum. First contour at $\ln(\mathcal{L}) = -1$ with respect to optimum, and subsequently at intervals of $\Delta \ln(\mathcal{L}) = 5$. (b) Optimal b_{iras} , showing tightly-controlled behaviour towards optimum at $b_{\text{iras}} = 1.04$. First contour at $b_{\text{iras}} = 1.0$, subsequently at $\Delta b_{\text{iras}} = 0.01$. (c) CMB-only $\ln(\mathcal{L})$, with degeneracy in $\{\Omega_m, h\}$ shown in the flat trough; contours as (a) above. (d) IRAS-only $\ln(\mathcal{L})$; contours as (a) above.

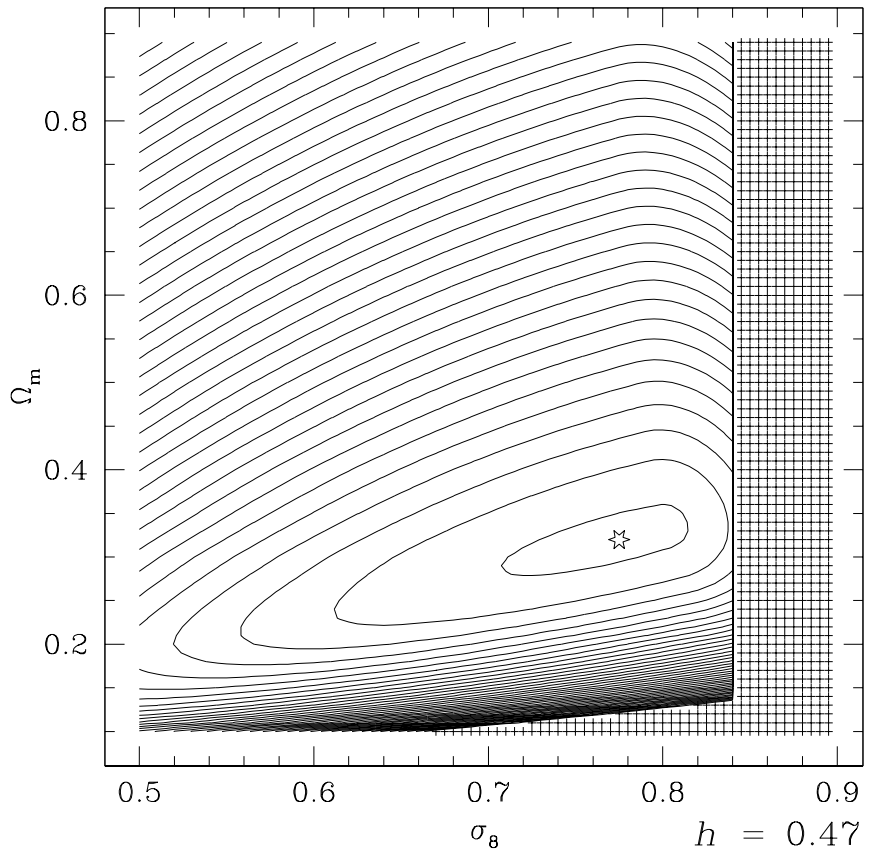


Fig. 3.— Joint likelihood, plotted on the $\{\Omega_m, \sigma_8\}$ plane at the optimal value of $h = 0.47$, with joint optimum marked at $\Omega_m = 0.32$, $\sigma_8 = 0.775$. First contour at $\ln(\mathcal{L}) = -1$ with respect to optimum, and subsequently at intervals of $\Delta \ln(\mathcal{L}) = 5$.

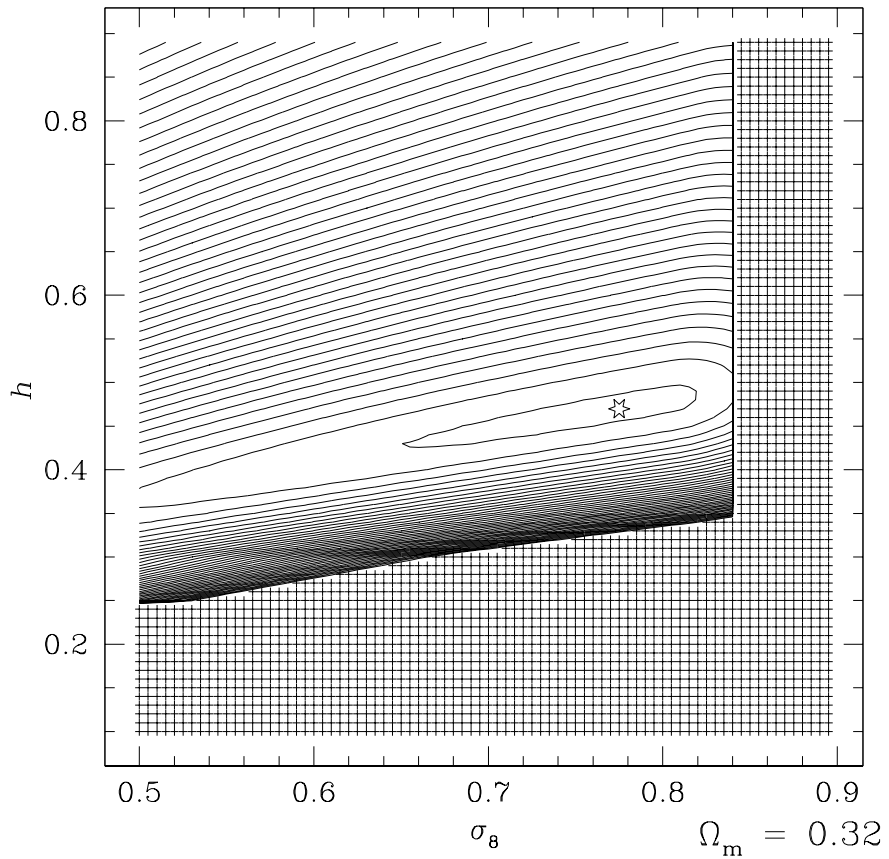


Fig. 4.— Joint likelihood, plotted on the $\{h, \sigma_8\}$ plane at the optimal value of $\Omega_m = 0.32$, with joint optimum marked at $h = 0.47$, $\sigma_8 = 0.775$. First contour at $\ln(\mathcal{L}) = -1$ with respect to optimum, and subsequently at intervals of $\Delta \ln(\mathcal{L}) = 5$.

Global Optimum	
Ω_m	0.32 ± 0.08
Ω_b	0.061 ± 0.013
h	0.47 ± 0.06
σ_8	0.78 ± 0.10
b_{iras}	1.04 ± 0.06
Q	17.14 ± 0.08
β_{iras}	0.48 ± 0.08
Γ	0.15 ± 0.08
$\sigma_{8,\text{iras}}$	0.81 ± 0.08

Table 1: Parameter values and standard errors for joint optimum. Optimal values are given with symmetrised 95% confidence limits, calculated for each parameter by marginalising the likelihood over the other variables.

	σ_8	h	Ω_m	Ω_b	b_{iras}
σ_8	1	0.21	-0.72	-0.11	-0.10
h	0.21	1	0.80	-0.71	0.06
Ω_m	-0.72	0.80	1	0.37	0.14
Ω_b	-0.11	-0.71	0.37	1	-0.03
b_{iras}	-0.10	0.06	0.14	-0.03	1

Table 2: Parameter correlation matrix at joint optimum

joint parameters, complete with error estimates. For each parameter, the error estimates are calculated by integrating the likelihood function over the other variables to produce a marginalised one-dimensional probability distribution. In general, the peak of the one-dimensional probability distribution for each variable will not coincide with the global optimum across all parameters. However, for all five variables in this system, the two values are found to be extremely close. Table 2 shows the correlation matrix for the parameters at the joint optimum. The reduced χ^2 for this set of parameters is 1.38, confirming that the results agree well with the models used.

The complementary nature of the two data sets is demonstrated in figure 2, which shows likelihood surfaces above the $\{\Omega_m, h\}$ plane at the optimal value of σ_8 . The fundamental CMB-side degeneracy in $\{\Omega_m, h\}$ is seen in the flat trough running across figure 2c. Combining this with the IRAS likelihood surface (figure 2d) breaks the degeneracy, leading to a very well-defined optimum (figure 2a). Similarly, combination with the CMB data allows estimation of b_{iras} , as shown in figure 2b. Figures 3 and 4 show joint likelihood surfaces above the $\{\Omega_m, \sigma_8\}$ and $\{\sigma_8, h\}$ planes respectively.

Recalculating the joint optimum using the simpler formula $\Gamma = \Omega_m h$ in place of that in equation 19 had little effect. Further, the optimum was robust to changes in IRAS l_{max} in the range $4 \leq l_{\text{max}} \leq 10$.

6. Discussion

The results of this joint optimisation are in reasonable agreement with other current estimates, and as such embody many of the problems inherent in our cosmological models.

The relatively low value of $\Omega_m = 0.32$ is close to that found by others (White et al. 1993, Bahcall, Lubin & Dorman 1995, Willick et al. 1997), and is in-line with recent supernovae results (Perlmutter et al. 1998). However, given the assumption of a flat universe, it requires a very high cosmological constant ($\Omega_\Lambda = 0.68$). Unfortunately, gravitational lensing measurements have constrained $\Omega_\Lambda \leq 0.50$ with 95% confidence (Maoz & Rix 1993, Kochanek 1996). Similarly, at this value of Ω_m , $h = 0.47$ agrees well with several other measurements (Sugiyama 1995, Lineweaver et al. 1997), but falls at the low end of the generally accepted range from local measurements (Freedman et al. 1994). The optimal baryon density, $\Omega_b = 0.061$ implies $\Omega_b h^2 = 0.0135$ —closer to the old estimate $\Omega_b h^2 = 0.0125$ (Copi, Schramm & Turner 1995) than to the new value from deuterium abundance, $\Omega_b h^2 = 0.024$ (Tytler, Fan & Burles 1996). Our value for the normalization $\sigma_8 = 0.775$ is relatively uncontroversial.

On the IRAS side, $\beta_{\text{iras}} = 0.48$ is in agreement with several other measurements (Strauss 1989, Schlegel 1995, Willick et al. 1997), although there is a family of others which place β_{iras} much higher (Dekel et al. 1993, Sigad et al. (in preparation)). Willick et al. 1997 discuss the discrepancies between the various measurement techniques, and why they lead to such distinct results. Finally, the IRAS mass to light bias is seen to be close to unity ($b_{\text{iras}} = 1.04$), suggesting

that the IRAS galaxies (mainly spirals) are good tracers of the underlying mass distribution.

The near future will see a dramatic increase in LSS data (e.g. the PSCZ, SDSS, 2dF surveys) and detailed measurements of the CMB fluctuations on sub-degree scale (e.g. from the Planck Surveyor and MAP satellites). Further work would lead naturally to broader and more accurate parameter estimation, untying the various parameters held fixed in the present optimisation. For example, permitting a tilted CDM power spectrum ($n_s < 1$) and a non-zero tensor CMB component might help reconcile the predicted Ω_Λ with lensing data. We should also bear in mind the possibility that future, more accurate measurements and analyses might lead to rejection of all current models.

Acknowledgments

We would like to thank Eric Gawiser, Kelvin Wu and Sarah Bridle for helpful discussions. Matthew Webster acknowledges a PPARC studentship. Graça Rocha acknowledges a NSF grant EPS-9550487 with matching support from the State of Kansas and from a K*STAR First award.

REFERENCES

Bahcall N.A., Lubin L.M. & Dorman V., 1995, ApJ, 447, L81

Bardeen J.M., Bond J.R., Kaiser N. & Szalay A.S., 1986, ApJ, 304, 15

Bennett C.L. et al. , 1996, ApJ., 464, L1

Bond J.R., 1995, *Cosmology and Large Scale Structure* ed. Schaeffer, R. Elsevier Science Publishers, Netherlands, Proc. Les Houches School, Session LX, August 1993

Bond J.R., 1995, Astrophys. Lett. and Comm., 32, 63

Bond J.R., Davis R.L. & Steinhardt P.J., 1995, Astrophys. Lett. and Comm., 32, 53

Carroll S.M., Press W.H. & Turner E.L., 1992, Ann. Rev. Astron. & Astrophys., 30, 499

Cheng E.S. et al. , 1994, ApJ., 422, L37

Cheng E.S. et al. , 1996, ApJ., 456, L71

Cole S., Fisher K.B. & Weinberg D.H., 1995, MNRAS, 275, 515

Copi C.J., Schramm D.N. & Turner M.S., 1995, Science, 267, 192

De Bernardis P. et al. , 1994, ApJ., 422, L33

Dekel A., Bertschinger E., Yahil A., Strauss M., Davis M. & Huchra J., 1993, ApJ, 412, 1

Efstathiou G., Bond J.R. & White S.D.M., 1992, MNRAS, 258, P1

Fisher, K.B., Scharf, C.A. & Lahav, O., 1994, MNRAS, 266, 219

Fisher, K.B., Huchra, J.P., Strauss, M.A., Davis, M., Yahil A., Schlegel D., 1995, ApJ, 100, 69

Fisher K.B. & Nusser A., 1996, MNRAS, 279, L1

Freedman W., Madore B., Mould J., Hill R., Ferrarese L., Kennicutt R., Saha A., Stetson P., Graham J., Ford H., Hoessel J., Huchra J., Hughes S. & Illingworth G., 1994, Nature, 371, 757

Gundersen J.O et al. , 1995, ApJ., 443 L57

Hancock S., Davies R.D., Lasenby A.N., De La Cruz C.M.G., Watson, R.A., Rebolo R., Beckman J.E., 1994, Nature, 367, 333

Hancock S., Gutierrez C.M., Davies R.D., Lasenby A.N., Rocha G., Rebolo R., Watson R.A., Tegmark M., 1997, MNRAS, 298, 505

Hancock S., Rocha G., Lasenby A.N., Gutierrez C.M., 1998, MNRAS, 294, L1

Heavens A.F. & Taylor A.N., 1995, MNRAS, 275, 483

Kaiser N., 1987, MNRAS, 227, 1

Kaiser N., Efstathiou G., Ellis R., Frenk C., Lawrence A., Rowan-Robinson M., Saunders W., 1991, MNRAS, 252, 1

Kochanek C.S., 1996, ApJ, 466, 638

Lahav, O., Fisher, K.B., Hoffman, Y., Scharf, C.A, & Zaroubi, S., 1994, ApJL, 423, L93

Lahav O., 1996, Helv. Phys. Acta, 69, 388

Lineweaver C.H., Barbosa D., Blanchard A. & Bartlett J.G., 1997, Astron. & Astrophys., 322, 365

Maoz D. & Riz H., 1993, ApJ, 416, 425

Netterfield C.B., Devlin M.J., Jarosik N., Page L., Wollack E.J., 1997, ApJ, 474, 47

Peebles, P.J.E., 1980, *The Large-Scale Structure of the Universe*, (Princeton: Princeton University Press)

Perlmutter S., Aldering G., DellaValle M., Deustua S., Ellis R.S., Fabbro S., Fruchter A., Goldhaber G., Groom D.E., Hook I.M., Kim A.G., Kim M.Y., Knop R.A., Lidman C., McMahon R.G., Nugent P., Pain R., Panagia N., Pennypacker C.R., RuizLapuente P., Schaefer B. & Walton N., 1998, Nature, 391, 51

Press, W.H., Teukolsky, S.A., Vetterling, W.T., & Flannery, B.P., 1992, *Numerical Recipes (Second Edition)* (Cambridge: Cambridge University Press)

Rocha, G., Hancock, S., Lasenby, A.N., Gutierrez, C.M. in preparation.

Ruhl J.E., Dragovan M., Platt S.R., Kovac J., Novak G., 1995, ApJ., 453, L1

Scaramela N., Vittorio N., 1990, ApJ., 353, 372

Scaramela N., Vittorio N., 1993, ApJ., 411, 1

Schlegel D., 1995, Ph. D. Thesis, University of California, Berkeley

Scott D., Srednicki M., White M., 1994, ApJ., 241, L5

Scott, P.F. et al. , 1996, ApJ., 461, L1

Seljak U., Zaldarriaga M., 1996, ApJ, 469, 437

Sigad Y., Dekel A., Strauss M.A. & Yahil A., 1998, in preparation

Smoot, G.F. et al. , 1992, ApJ., 396, L1

Strauss M.A., Ph. D. Thesis, University of California, Berkeley

Strauss M.A., Davis M., Yahil A. & Huchra J.P, 1992a, ApJ, 385, 421

Strauss, M.A., & Willick, J.A., 1995, Phys Rev, 261, 271

Sugiyama N., 1995, ApJ Supp., 100, 281

Tanaka, S.T. et al. , ApJ, 468, L81

Turner M.S., Truran J.W., Schramm D.N. & Copi C.J., 1996, ApJ, 466, L59

Tytler D., Fan X.M. & Burles S., 1996, Nature, 381, 207

White et al. , 1993, Nature, 366, 429

Willick J.A., Strauss M.A., Dekel A. & Kolatt T., 1997, ApJ, 486, 629

Yahil, A., Strauss, M.A., Davis, M., & Huchra, J.P., 1991, ApJ, 372, 380